Molecular layers of a polymer at the free water surface : microscopy at the Brewster angle

E. Mann, S. Hénon, D. Langevin, J. Meunier

Classification
Physics Abstracts
68.15 — 07.60 — 47.90

Molecular layers of a polymer at the free water surface : microscopy at the Brewster angle

E. K. Mann, S. Hénon, D. Langevin and J. Meunier

Laboratoire de Physique Statistique de l'E.N.S. (*), 24 rue Lhomond, 75231 Paris Cedex 05, France

(*Received 24 January 1992, accepted in final form 18 June 1992*)

Résumé. — La microscopie à l'angle de Brewster, récemment développée pour visualiser les couches monomoléculaires sur les surfaces liquides sans ajouter de sondes fluorescentes, est utilisée pour étudier les couches moléculaires d'un polymère, le poly(dimethylsiloxane), à l'interface eau-air. La coexistence de domaines de densité de surface différente est observée, à la fois aux basses concentrations et aux concentrations au-dessus du collapse de la monocouche. Les domaines isolés sont ronds quand ils sont petits ; les temps de relaxation de domaines déformés sont mesurés. Ces temps de relaxation, couplés aux très basses viscosités de surface déduites d'autres mesures, suggèrent que les tensions de ligne sont très faibles. De petits changements dans les conditions expérimentales peuvent entraîner la déstabilisation des parois des domaines.

Abstract. — A recently developed microscope, allowing the visualization of monolayers at liquid surfaces without the addition of fluorescent molecules, is used to study molecular layers of a polymer, poly(dimethylsiloxane), on water. Coexistence of domains of different surface density is observed, both at low concentrations and at concentrations above collapse. Small isolated domains are circular ; characteristic relaxation times for a deformed domain are measured. These relaxation times, coupled with the very low surface viscosities previously measured, suggest very low line tensions ($\sim 10^{-13}$ N). Small changes in experimental conditions can result in the destabilization of domain borders.

Introduction.

Within the last ten years it has become possible to directly visualize monomolecular films of amphiphilic molecules, in particular such inhomogeneities in films as are found at first order phase transitions. A variety of standard monolayers have been studied including fatty acids, esters and phospholipids as well as mixed monolayers. In combination with other methods, such as X-ray scattering and a return to careful surface pressure measurements, an unexpected richness of possibility for the behavior in monomolecular films has been revealed [1]. A multiplicity of domain shapes are observed, including simple circles, vague hexagons,

(*) URA 1306 du CNRS, associée aux Universités Paris VI et VII.

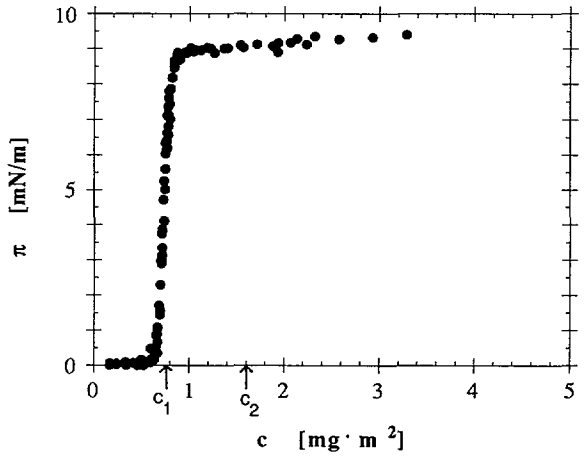

Fig. 1. — Surface pressure for PDMS on water, as a function of PDMS surface concentration.

two-dimensional foams, spiral and branched shapes, and labyrinthine structures. The order and form of the domains are strongly suggestive of the presence of long range forces, largely ignored previously [2].

Certains polymers also form monomolecular films on the water surface. Such polymers as poly(dimethylsiloxane) (PDMS) and poly(methylmethacrylate) (PMMA) form condensed films, with very low surface pressures below concentrations approaching a characteristic value here called c_1 ; numerically this corresponds to saturation with a dense layer of monomers each adsorbed on the liquid surface, though it is only recently that such a layer could be demonstrated directly, with neutron reflectivity studies [3]. Near c_1, the surface pressure rises abruptly to a plateau value (see Fig. 1 for the PDMS case), where it is said that the monolayer collapses. Since the surface pressures are ummeasurably low until c_1 is approached, lower than predicted by the ideal gas law (where that is itself measurable), it has been suggested that the polymer forms island domains, that is that phase segregation occurs. Reflectivity measurements revealing inhomogeneities in the surface of such monolayers support this interpretation [4, 5]. This is particularly clear in recent ellipsometry measurements on PDMS, which imply very large domain sizes, greater than the 2 mm field of observation [4].

The configuration of the polymer above the collapse concentration is unclear, as indeed for any other molecule. Since we are dealing with a polymer, it may remain monomolecular in the film but take on some different configuration, for example changing from flat on the surface to coiled in a helix, the standard model since the 1950's for the case of PDMS [6]. Bulk three-dimensional domains may form, in coexistence with a basic monolayer, according to the usual model for the collapse of a surfactant monolayer. The possibility of multilayer formation is suggested by recent experiments in which PDMS was spread on dry surfaces ; the central droplet developed steps, with heights of approximately monomer size [7]. The ellipsometry study cited above [4] found fluctuations at high concentrations, implying at least highly inhomogeneous films on water ; some structuration in discrete thicknesses was suggested. Clearly direct visualization of the polymer film is highly desirable, to clarify the behavior at both high and low surface concentrations.

Fluorescence microscopy was the first direct method for such visualization [8, 9]. Fluorescent probes in a monolayer at the liquid surface distribute differently in different phases, yielding a contrast between the phases. The effect of this impurity on the monolayer state is unknown, but can be minimized by minimizing the probe concentration [10]. The

probe is nearly completely expelled from relatively dense phases, eliminating visual contrast ; the nature of any denser phase and any collapse into three dimensions cannot be explored. In an alternative approach, the properties of a fluorescent amphiphile at a surface is itself studied ; the molecule will not have the same properties as its non-fluorescent counterpart but can be interesting in itself [11].

The Brewster angle microscope [12] was developed to observe directly such inhomogeneous surfaces without the use of fluorescence, or any other probe. It is used here to investigate molecular layers of PDMS, both below and far above the saturation concentation. In both cases, a separation into domains of contrasting, constant thicknesses was observed. At high concentrations, within the collapse regime, coexisting domains with as many as three distinct thicknesses were seen, in the presence of much thicker droplets. Superstructures in the form of stripes or two-dimensional foams were observed in the two cases, as well as more compact domains, significantly deformed in the presence of other domains.

In the midst of this diversity, in both concentrations regimes, small isolated domains were circular, and if deformed (mechanically at sub-monolayer concentrations, after coalescence of two domains in the very high concentration "collapse" regime where such coalescence occurred), were observed to relax to circles. Within experimental limitations, given by the rather long sampling time (3.5 s) and the limitations on observation time ($<$ 15-30 s), the relaxation was exponential. The charecteristic exponential relaxation time of these domains was studied as a function of radius r (5 μm $< r <$ 100 μm) for two different molecular weights of the polymer.

Such relaxation suggests a line tension restoring force balanced by viscous effects ; the dependence of the relaxation times on the size of the domains suggests that the viscosity within the polymer film plays the determining role. The line tension can be estimated at $\sim 10^{-13}$ N.

Method.

The reflectivity of a plane interface between two media (refractive index n_1 and n_2) depends on the polarization and angle of the incident light. At the Brewster angle θ_B ($\tan \theta_B = n_1/n_2$) and for polarization p (electric field in the plane of incidence) this reflectivity is zero for an ideal plane interface, that is, one without thickness, roughness, or anisotropy. Any finite reflectivity at this angle and polarization is due to departures from this ideal, and is therefore very sensitive to interfacial structure. For this reason the classic method of ellipsometry, which can give quantitative information about such structure, averaged over the field-of-view and limited mainly by the difficulty in disentangling the different effects, is often performed at this angle on very thin films. The Brewster angle microscope, described in detail elsewhere [12], uses the same property of the Brewster angle on a local level, to observe coexisting domains of separate phases, with differing thickness or optical anisotropy.

This microscope is used in a dynamic mode to follow relaxation times of domains as well as other evolutions in time of the monolayer. The minimum time between images in 3.5 s, the rather long time interval dictated by the necessity of taking each image as a series of bands (since the image is only in focus along a band for a given distance between the camera objective and the surface) joined edge-to-edge. Since the field-of-view is swept in alternating directions, only the center of the image is separated by equal time intervals, with oscillations around the average at the top and bottom of the image. The field-of-view is limited to 600 μm by the beam size, minimized for maximum intensity ; the Gaussian illumination is visible on the images.

PDMS of three different molecular weights, including both narrow weight fractions and polydisperse samples, were used in these preliminary studies : $M_w = 10.000$ (a.

$M_w/M_n = 1.13$, monomode [13], b. Rhône-Poulenc, 47 v 100 $M_w/M_n = 1.8$; treated to remove low-weight oligomers) ; $M_w = 33.000$ (Rhône-Poulenc, 47 v 1 000 $M_w/M_n = 2.4$) and $M_w = 101.000$ ($M_w/M_n = 1.23$, monomode [13]). The concentration of polymer on the surface was varied by the method of successive addition using hexane or chloroform spreading solutions. The substrate was ultra-pure water treated by a Millipore-Milli Q system.

Results.

The qualitative elements of the morphology observed in the two different concentration regimes, submonolayer (average polymer surface concentration $c < c_1$) and collapse ($c > c_2 \sim 2\ c_1$), are presented in the first two subdivisions of this section. The quantitative relaxation of small domains in both concentration regimes, and the relation of this relaxation to a line tension, is presented in a third subsection. The possibility of relating the estimated line tension to the observed morphologies is also discussed.

OBSERVATIONS, SUBMONOLAYER CONCENTRATIONS ($c < c_1$). — The ellipsometric results in reference [4], reproduced in figure 2, strongly suggest lateral phase separation into dense and very dilute domains in this regime. Either ellipticities characteristic of pure water or ellipticities characteristic of a polymer layer may be observed, but not fluctuations between the two as would result from an average over the 2 mm reflected beam. This behavior suggests very large domains, with the border between two domains far from the observation point.

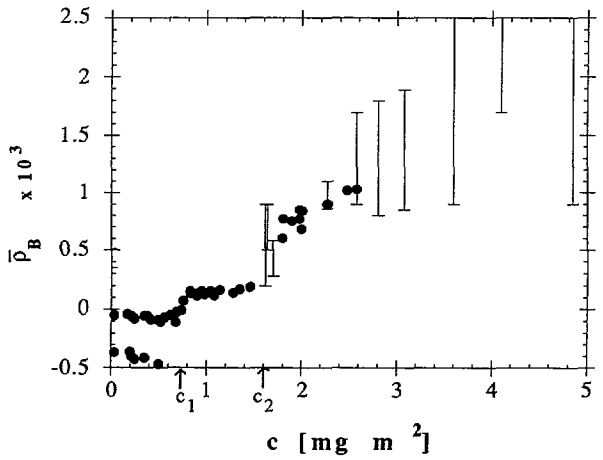

Fig. 2. — Ellipticity for PDMS on water, as a function of PDMS surface concentration. The ellipticity $\bar{\rho}_B$, measured at the Brewster angle, is the ratio of the reflected amplitudes for the field components polarized respectively parallel and perpendicular to the plane of incidence. The bars correspond to the range of observed ellipticities.

Direct visualization of such domains by the Brewster microscope confirms this hypothesis : under the same experimental conditions as applied for the ellipsometry, and by carefully selecting the field of observation on the surface, it is possible to see a domain boundary between a dense and a dilute phase as in figure 3a. The limited field of the microscope means that the careful placement on the surface is crucial : otherwise nothing is observed except perhaps a band of different brilliance passing in the early minutes after deposition. The

« correct » placement to observe a border appears to be consistent with the segregation of most of the polymer in a single domain, approximately centered in the dish. Notice also the scale of the image and the very slight curvature of the domain boundary, implying domains of at least several millimeters.

To determine which of the two phases is dense in polymer, refer back to the ellipsometric data : the phase dense in polymer reflects *p* polarized light less than the pure water surface, as the contribution to the reflectivity due to the polymer layer nearly exactly cancels that due to the roughness of the surface (the ellipticity is near zero for a monolayer in Fig. 2) ; it is the dark regions on the images that are dense in polymer. This is confirmed by direct observation ; although the extreme inhomogeneity of the surface makes it difficult to estimate the proportion of dark surface at a given polymer concentration, this clearly increases from null to dominant as the layer approaches saturation. The reason for the limited image quality becomes clear : a water surface is very nearly the perfect smooth, abrupt interface which would be entirely non-reflecting, and this is the brighter of the two phases in the submonolayer regime.

Methods for the direct visualization of monolayers on liquid surfaces have only become available in the last several years. A great variety of domain shapes are observed, including 2-d foams, spiral-shaped domains and labyrinthine structures. The surfaces are typically very heterogeneous, including both very large and very small domains, whose shapes are very sensitive to experimental conditions, including the method of deposition of the layer, the presence of any impurities, temperature and changes in temperature, and possibly humidity [1, 14, 15]. The case of PDMS is no exception.

Very large, possibly single, domains are seen when the surface is carefully enclosed, that is protected from disturbing air currents and with the atmosphere saturated in humidity ; these were also the conditions of the ellipsometric study. When the cover is removed, the humidity is greatly reduced, leading to evaporation (impeded by any monolayer, and thus inhomogeneously on an inhomogeneously covered surface), reducing the surface temperature. Further, any air currents disturb the surface. Under these conditions, a wide variety of domain shapes is observed on an extremely inhomogeneous surface. Smaller domains cluster near the edge of much larger ones (Fig. 3b). Domains are considerably deformed in the presence of nearby domains, even at several microns separation (Fig. 3c). Two-dimensional foams are observed (Fig. 3d), as with fatty acids, for example [15].

As with more separated domains, the foams observed here are considerably deformed from the canonical case : note in image 3d that in some cases more than three bubbles seem to meet at a corner and that the angles at the intersection of bubbles are not necessarily 120°. This may simply reflect slow relaxation times of the network to an equilibrium configuration. It was not possible to properly follow the foam with time because it coarsens, similarly to any three-dimensional foam and as studied in other monolayer systems using fluorescence microscopy (which allows a free adjustment of the field size) [15], and quickly reaches characteristic sizes larger than the maximum field-of-view, limited by the size of the laser beam. The indication is that cells in the network elongate with time, along the direction of the movement of the monolayer under light air currents.

Aside from such apparently dynamical effects, very elongated domains, in the form of stripes, are observed on the surface (Figs. 3e, f). Such stripes are generally taken to reflect a competition between line tension, favoring round domains, and longer ranged forces of electrostatic origin, which favor elongated domains : under these conditions very large domains are expected to form stripes while much smaller domains remain circular. With some knowledge of the competing forces a limiting size can be calculated, below which domains are round [16, 17].

A critical radius R_c cannot be determined from our observations : domains fitting within the field-of-view of the microscope are seen only in the absence of the cover, when such factors as air currents may intervene. Even in this case, domains are deformed in the presence of other domains and further, the images certainly do not represent an equilibrium situation. The

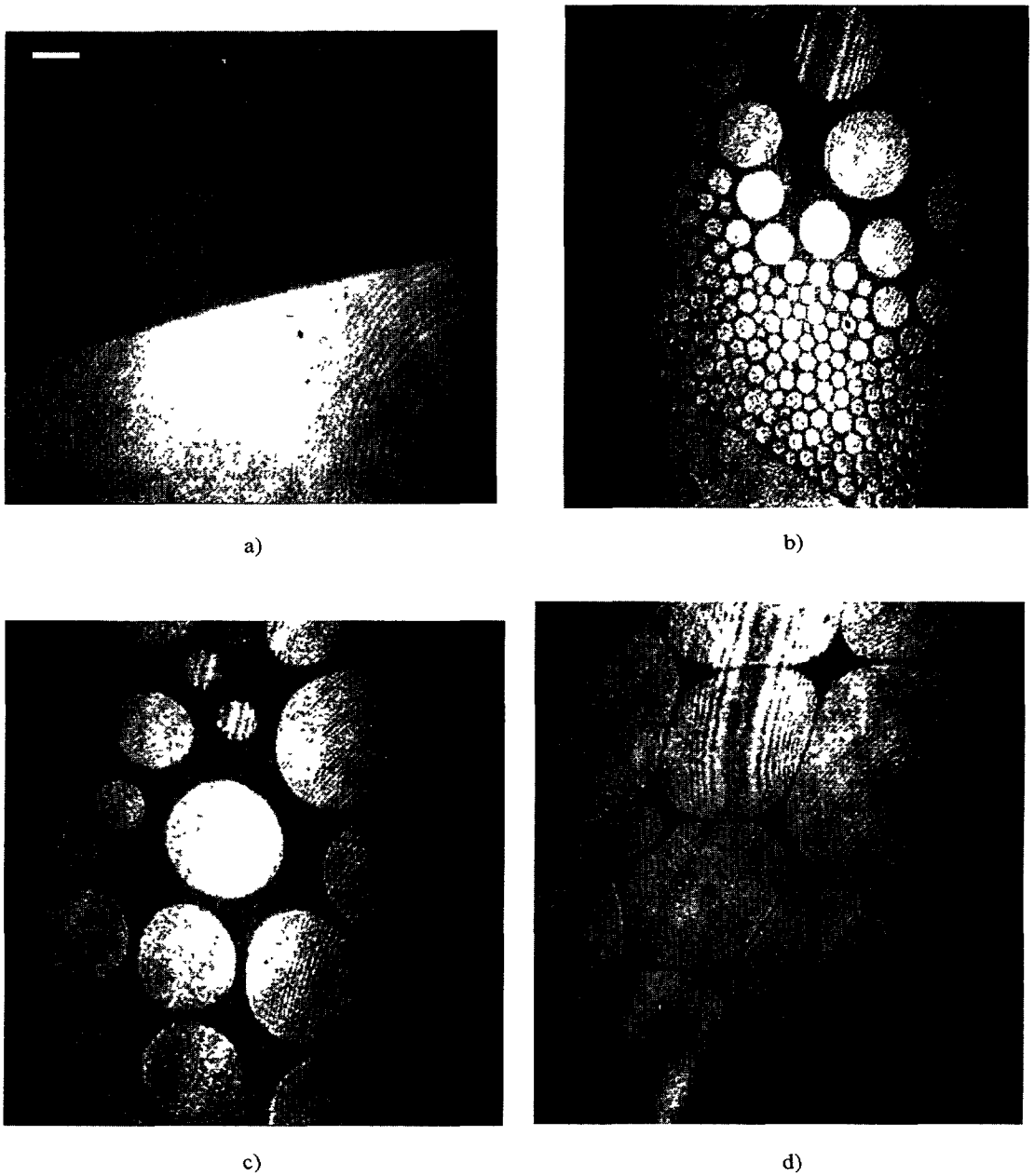

Fig. 3. — Images : PDMS on water in the submonolayer regime ($c < 0.5$ mg/m^2) [see text]. Dark regions are dense in polymer, bright regions dilute in polymer (see Fig. 2 and text). All bars on images correspond to 50 μm. The Gaussian illumination is visible on the images.

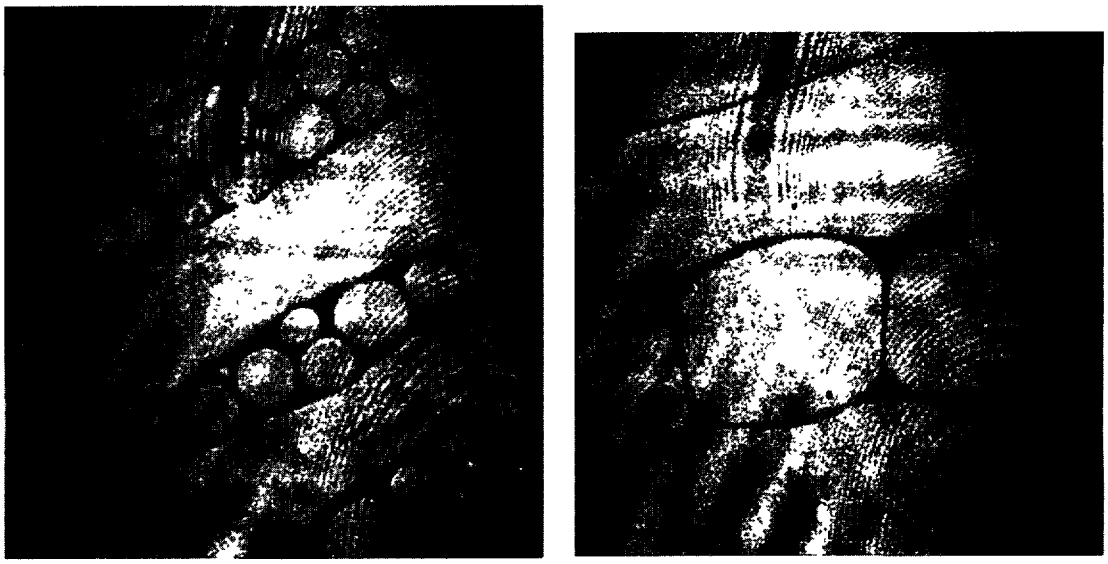

Fig. 3 *(Continued).* e) f)

mutual deformation of domains even at a distance of several micrometers and the absence of coalescence between domains does suggest the possibility of long-range repulsion, and it would be interesting to quantitatively evaluate any such effect for comparison with the observed morphologies, which imply $R_c \geq 100$ μm.

It is difficult to deduce the electrostatic forces directly from molecular quantities, noting for example that the silicon-oxygen bond in the polymer molecule has an associated dipole moment of 2.8D [18], because the force depends very sensitively both on the detailed orientation of the molecule within the interface and on the dielectric constant as it varies through the interfacial region. Neither of these is known. However, the surface potential also depends on these factors and it is argued (in an appendix) that in a laterally isotropic phase of dipolar molecules at a dielectric interface, the long-range eloectrostatic forces can be directly related to the measured surface potential. Measurements for the surface potential of the polymer PDMS on water, existing in the literature [6, 19], then lead to a relation between the critical radius R_c and the line tension (see Appendix). A critical radius of 100 μm would correspond to a line tension $\lambda = 2 \times 10^{-13}$ N, a very small value, with comparisons to be discussed below. If λ is of this order, such long-range interactions may explain the stripe domains observed, but these may equally be due to dynamic effects and long relaxation times from the configurations imposed by the initial deposition of the layer and any disturbance of the surface. An independent estimate of the line tension is necessary for any further evaluation of the possibilities. Such an estimate will be presented shortly.

All of these measurements are necessarily made in the absence of the cover. With the cover enclosing the sample cell, protecting it from air currents and ensuring a high humidity, domains are much too large to fit within the field-of-view of the microscope. Without the cover, the varied domains described above appear. If the cover is replaced, small isolated bright domains (holes in the monolayer) disappear, beginning after a delay of several seconds but then proceeding quickly, so that domains of about 20 μm disappear within about 5 s. The process is much slower for such domains near much larger ones.

The result can be even more dramatic if the monolayer has first been left uncovered to sit and develop for a certain time. With time, striped regions, similar to those observed soon

after deposition but of much larger extent, tend to develop ; figure 4a shows a typical example, 15 h after deposition of the monolayer and just after the dish has been covered. The initial effect of the cover is a decrease in the area of the brigth regions as before, but at later times the border between domains may destabilize as shown in figures 4b and 4c. This takes place essentially simultaneously over large regions of the film, as becomes obvious as the liquid surface moves through the field-of-view. If the cover is left on the cell, the labyrinthine pattern can continue to develop to below the one micron resolution of the microscope. In the run shown, the cover was removed before this point, completely reversing the process (Fig. 4d). If the labyrinth thins below one micron before uncovering, the bright domains reappear as much smaller broken segments ; these join to form a striped domain pattern very similar to the initial one, but on a finer scale. Marangoni effects due to temperature gradients in the surface would lead to fingering as observed [20], but here the fingering occurs when the cover is placed on the cell, and any temperature gradients reduced. The reforming of the long stripes from smaller domains upon reversing the process suggest that equilibrium effects are involved.

Similar labyrinth formation has been observed in other monolayer systems, again under dynamic conditions [21, 22]. Complicated hydrodynamical effects such as were just mentioned must be considered, but the morphological similarity to labyrinths formed in thin magnetic layers has led to the interpretation of such structures in terms of competing electrostatic and line tension forces. In the absence of any real estimate of these, evaluation of this hypothesis has been difficult.

While the estimation of these factors to be presented here can allow some such evaluation, the nature of the effect of the cover on the sample remains unclear. It can be noted that when conditions are near those favoring such a destabilization of form, small perturbations can have great influence : for example in reference [21] it is noted that near the shape transition, the light source could trigger this destabilization, it is assumed *via* a photochemical effect. This is certainly not true in our case : not only would this be difficult to relate to the reversible effect of the cover and the lower sensitivity to the probing light intrinsic to the technique used (one of the major advantages of the Brewster microscope over fluorescence microscopy), but destabilization develops simultaneously both at and well away from this probe. Other subtle effects may be involved. Further studies are under way to clarify the nature of the process, and in particular to determine if the impurity level in the layer upon sitting some 15 h plays an essential role, for example lowering λ. To date, the destabilization has only been observed with a polydisperse sample (Rhône-Poulenc 47 v 100), though observations on other samples are not yet sufficiently systematic to rule out the possibility.

OBSERVATIONS, HIGH CONCENTRATIONS $> c_2$. — At high concentrations, in the traditional collapse regime, coexisting domains of constant thickness are again observed, with some differences. First and trivially, the brightness of the layer increases with layer thickness ; a saturated monolayer corresponds to a reflectivity at the Brewster angle of nearly zero (refer to the ellipticity curve in Fig. 2) and increasing surface density increases the reflectivity. More fundamentally the spreading solutions, while good solvents for the polymer, are clearly ineffective in spreading it : on the dark background, the initial images show only brilliant points, with a diameter less than the resolution of the microscope (~ 1 μm), but by that brilliance, of thickness much greater than molecular. They are distributed very inhomogeneously on the surface, with sharp demarcations between regions dense and dilute in these points (Fig. 5a). The configurations observed depend on the concentration of the polymer in the spreading solutions as well as the final average concentration on the surface.

For dilute spreading solutions ($c \leq 0.05$ mg/ml), the initial brilliant points are relatively small. After 30-60 mn a homogeneous film may spread out from these points ; this spreading

a) b)

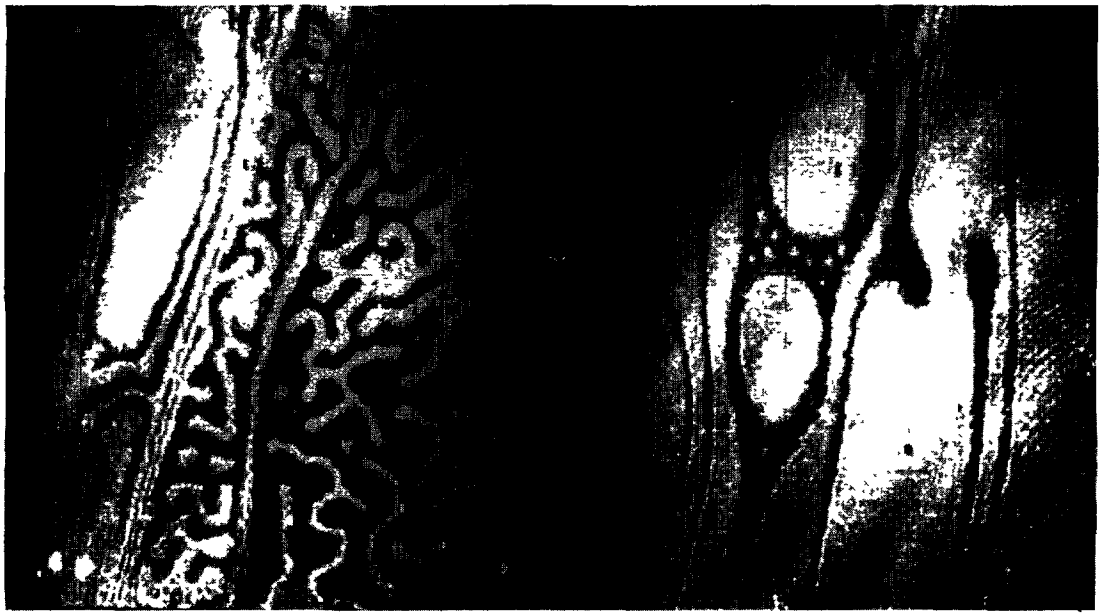

c) d)

Fig. 4. — Destabilization of domain boundaries after covering cell. $c = 0.3$ mg/m^2. a) add cover + 25 s. b) + 250 s. c) + 400 s. d) remove cover, + 150 s.

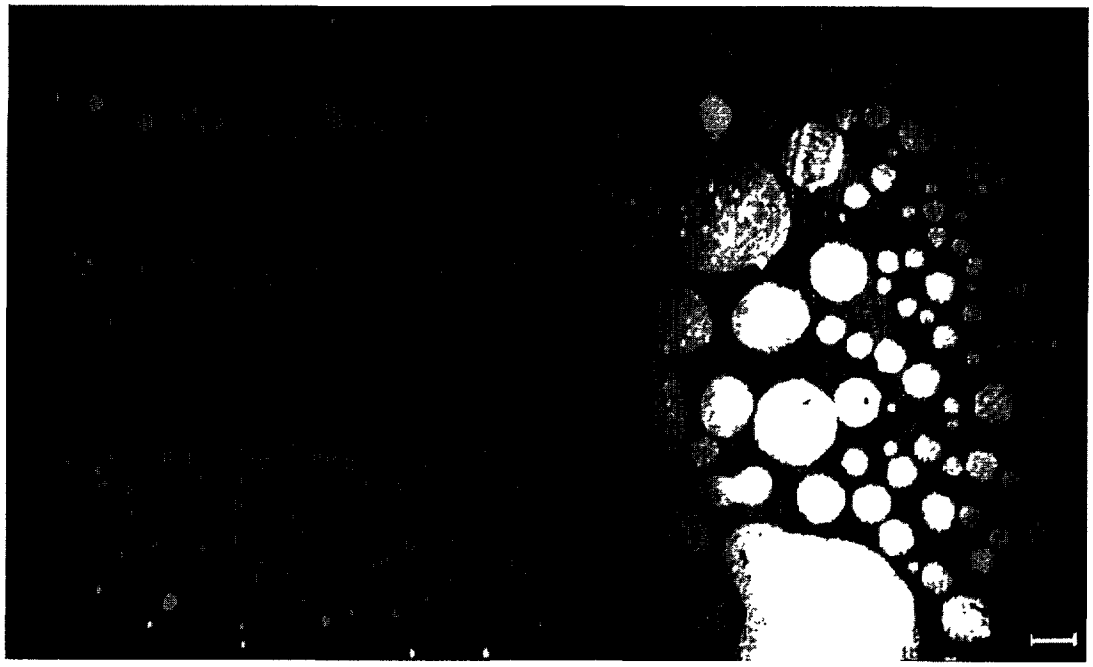

a) b)

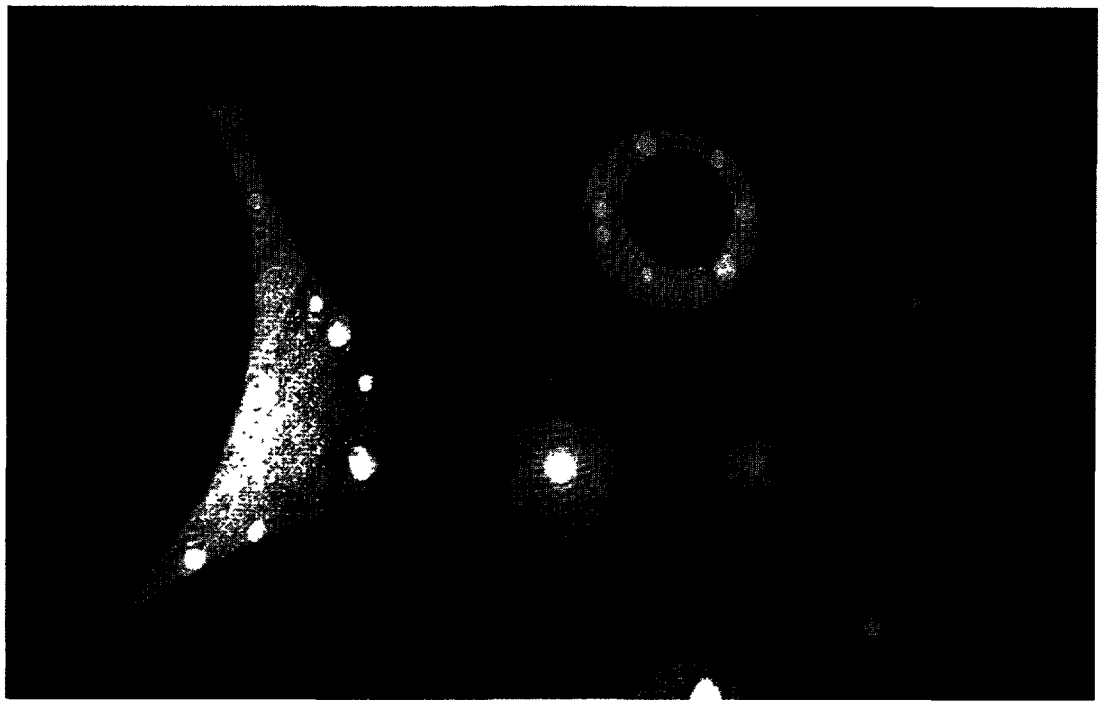

c) d)

Fig. 5. — Images, PDMS on water in the collapse regime, $c \sim 4$ mg/m^2 [see text]. Bars correspond to 50 μm. Bright regions are of higher polymer density than dark regions.

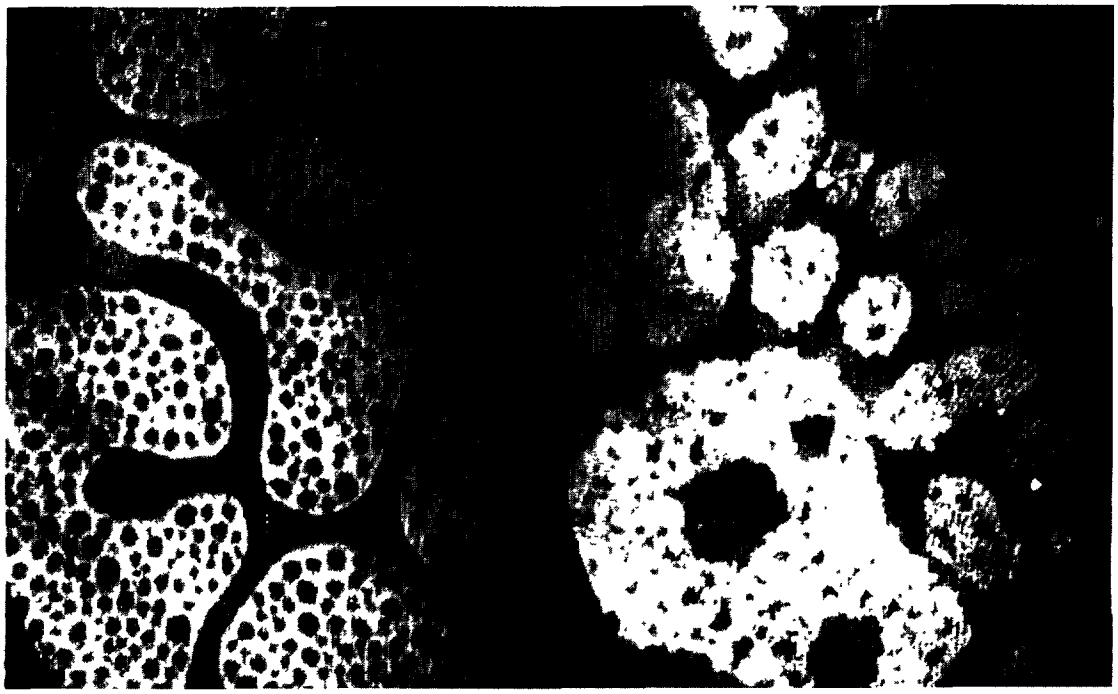

e) f)

Fig. 5 *(Continued).*

occurs relatively rapidly, and the domains may attain a diameter of 10 μm or more within a minute. These domains, if sufficiently close, coalesce (Fig. 5b) ; the new domains relax to circular forms over a period of about 10 s. This occurs both with and without the cover in place.

For slightly higher concentrations of polymer in the spreading solution ($c \sim 0.1$ mg/ml), similar patterns are observed, but initial points are more brilliant and form larger domains upon spreading, as may be seen in figures 5c and 5d. Macroscopic domains of at least two very different thicknesses may be seen on the dark background ; it is difficult to capture images since laser intensities sufficiently strong to observe one domain badly saturate the camera with the more brilliant domains. With yet higher concentrations of polymer in the spreading solution ($c \sim 0.5$ mg/ml), very brilliant uniform domains are observed in addition to the usual points immediatly after the polymer is spread ; again much thinner films are observed in the same film.

All images in this surface concentration regime show brilliant points, less than the 1 μm resolution of the microscope in diameter but much thicker than monomolecular. The spreading solution is not effective to fully spread the polymer, though the polymer is clearly capable of spreading to form films of various molecular thicknesses, and the more concentrated the solution, the larger the clumps of unspread polymer. The initial configuration of the polymer layer is thus highly dependent on the spreading solution, as has long been assumed for protein monolayers for example, and equilibration times are very slow. The brilliant points persist for at least 24 h, as long as the surface can reasonably be observed.

The influence of any retention of the spreading solvent may be tested by dispensing with it altogether, beginning with a drop of pure polymer and vacuuming the surface until molecular

thicknesses are attained. Results are similar : macroscopic droplets of the polymer which may spread, with coalescence of the resulting domains, as well as coexisting films of several different thicknesses.

Energy barriers between different film configurations appear small. Destabilization of film boundaries similar to what has been observed at sub-monolayer concentrations can occur even without obvious external influence (Figs. 5e, 5f).

RELAXATION TIMES. — While many different forms of domains can be observed, small isolated domains are essentially round in the two concentration ranges. Elongated domains are observed to relax to circles over a period of several seconds, a time (barely) accessible to the dynamic capabilities of the microscope.

At less than saturation concentrations, disturbing the surface elongates domains as well as produces new ones ; the difficulty lies in doing this in such a way that the domains do not move excessively as they relax, and in that sufficiently isolated domains are in general observed only in narrow border regions between areas essentially saturated and essentially free of polymer (Fig. 6a). The relaxation (Figs. 6a, 6b) of both dark and bright domains can be observed, that is, domains dense and dilute in polymer. The area of the dark (dense) domains remained constant during the relaxation, to within the precision of the measurement of ~ 10 %. Certain of the bright, polymer-free domains decreased in area by a factor of this

a)

Fig. 6. — Relaxation in submonolayer regime, $c \sim 0.45$ mg/m^2 : a) Typical domain pattern after stirring surface. b) Relaxation of a single dense domain with time, 3.5 s/frame. Bars correspond to 50 μm.

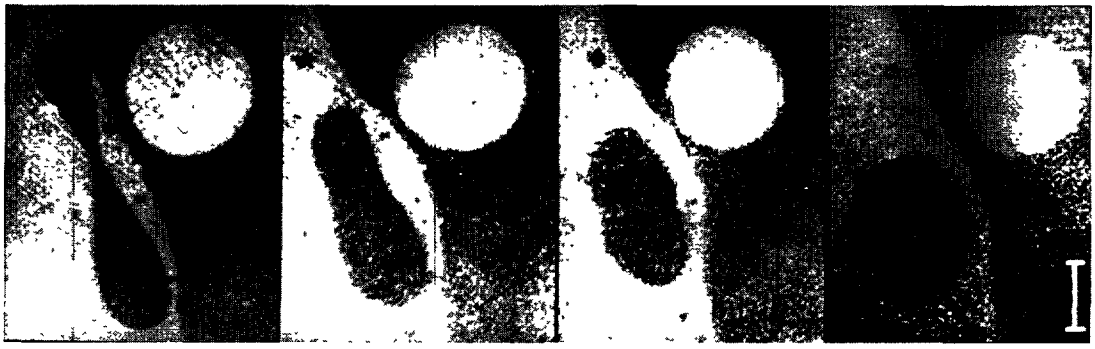

b)

Fig. 6 *(Continued).*

order during the course of the measure, but comparison of different domains suggests that this did not change the measured relaxation time, to within the 10 % precision largely limited by the movement of domains during the measurement.

In the high concentration collapse regime, the coalescence of two circular domains (which does not occur in the submonolayer regime) provides a natural opportunity to observe the relaxation of the subsequent larger domain (Fig. 7). Domains are intially quite monodisperse in a given region, but the continuation of the coalescence process can provide data for a range of domain sizes (Fig. 5b). The domain size was constant during the relaxation, again within the precision of the measurement.

a) b) c) d) e)

Fig. 7. — $c \sim 5$ mg/m^2. Coalescence of two dense domains in the collapse regime, followed by the relaxation of the resulting single domain. 7 s/frame.

The range of characteristic times that could be observed was limited from below by the minimum time between images (3.5 s) and from above by the maximum time in which a domain could be held within the field of view, roughly 15 s after the direct deformation of the monolayer and about twice that for the coalescence in the high concentration range (when the cover, providing protection from any air currents, could be kept in place without the disappearance of the domains under question). The size of the domains imposed a further limitation : the resolution of the microscope is 1 μm, while for larger domains the deformation of the image near the borders of the image is more important over the size of the domain. Note that the major limitation on the precision of the measurement is the relatively long time over which the image is taken : any movement of the domain during this period falsifies the deformation (as well as limiting the time over which the domain can be observed, before it leaves the field of view). This is very clear when the movement is steadily parallel to

the direction in which the images were taken (sweeping forwards and back), as was the case in the coalescence experiments : domains were observed to be alternatively elongated and contracted in that direction. Some correction may be made in this case.

To quantify the relaxation in either case, we use a very simple measure of the deformation from a circle : $\Theta = (L/W) - 1$, where L is the length and W the width of the domain as shown in figure 8. For not-too-large deformations, and within the precision of the measurement, Θ diminishes exponentially with time ($\Theta = \Theta_0 e^{-t/T_c}$) as demonstrated in figure 9 for three different domains in the case of coalescence at high concentration.

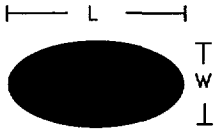

Fig. 8.

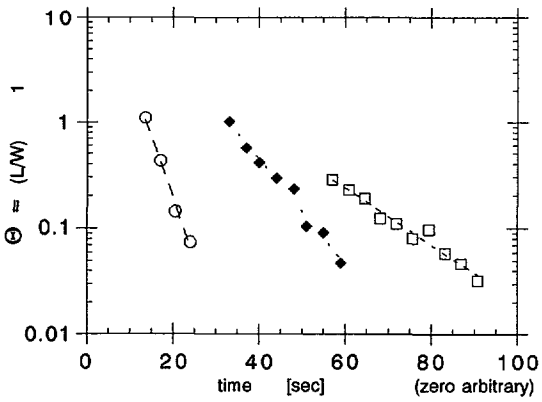

Fig. 9.

Fig. 8. — A definition for the distortion of a domain : $\Theta = \frac{L}{W} - 1$.

Fig. 9. — Relaxation after coalescence, $c \sim 5$ mg/m^2. Three different domains of radius (○) 7.5 μm ; (◆) 23 μm ; (□) 33 μm.

The characteristic time T_c of this relaxation is seen to be a function of the size of the domain, characterized by its mean radius $R \equiv (\text{Area}/\pi)^{1/2}$. This characteristic relaxation time is shown for the two concentration regimes in figures 10a and 10b. In the two cases T_c is approximately linear in R, with scatter that is generally within the precision of the measure. The low-concentration regime is particularly difficult, both because of the inherent irregular movement of the surface and also because there are always domains sufficiently nearby that independence is not necessarily a valid assumption.

The observation of such relaxation suggests the action of a line tension, that is, that the energy of a domain is minimized by minimizing its boundary : in a first assumption the line energy is $E_1 = \lambda \ell$ where λ is the line tension and ℓ is the length of the perimeter. The assumption that the energy associated with a boundary depends only on its length amounts to assuming that the forces involved are short-ranged. Long-ranged electrostatic forces would renormalize this line tension, depending on the size of the domains involved. For sufficiently large domains, the equilibrium shape would be elongated, eventually into a striped phase with a characteristic domain width. For the small domains considered here, the only expected effect of the long-range forces is the renormalization of the line tension, which may therefore decrease with increasing R [2, 22].

By Laplace's law, the presence of a line tension provides a restoring force, inversely proportional to the radius of curvature of the boundary. To produce an exponential

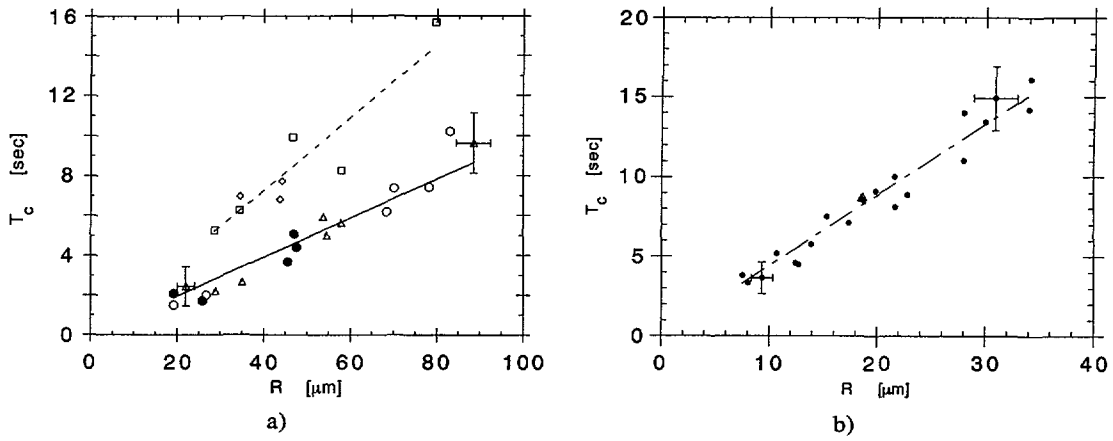

Fig. 10. — a) Characteristic relaxation time as a function of radius, submonolayer regime ($c \sim 0.45$ mg/m^2), for polymer samples of different molecular weight and polydispersity : M_w = (△) 10.000 ; (◆) 10.000* ; (□) 33.000* ; (○, ●) 101.000. (* refers to polydisperse samples.) Closed symbols are dark domains, dense in PDMS, open symbols bright domains, dilute in PDMS. Representative estimated error limits are shown on two data points. Solid line : fit, monodisperse samples, $T_c/R = 0.098$ s/μm. Dashed line : fit, polydisperse samples, $T_c/R = 0.18$ s/μm. b) Characteristic relaxation time after coalescence in collapse region ($c \sim 4$ mg/m^2). M_w = (△) 10.000* ; (●) 101.000. (* refers to polydisperse sample.) Representative estimated error limits are shown on two data points. Line : fit, $T_c/R = 0.44$ s/μm.

relaxation, this line tension is opposed by dissipation during the movement ; *a priori* there are three viscosities involved here :

— υ_s the surface shear viscosity of the polymer layer ;
— υ_b the shear viscosity of the substrate which may move with the polymer layer ;
— υ_{s-b} the viscosity between the film and the substrate.

The hydrodynamics are nontrivial, even if we assume that inertial effects can be ignored, as is reasonable given the purely exponential decay. As a first approximation consider only the surface shear viscosity. Dimensional arguments suggest directly

$$T_c \sim R \frac{\upsilon_s}{\lambda},$$

in analogy with the relaxation of distorted drops in three dimensions [23]. Indeed this correlates well with what it is observed ; other viscosity contributions should lead to higher orders of R appearing. If the substrate viscosity becomes important,

$$T_c \sim R^2 \frac{\upsilon_b}{\lambda}.$$

Significant motion of the domain with respect to the surface, involving υ_{s-b}, is not expected even in the case of multiple layers since this would involve enormous dissipation. Characteristic times would be similar to those observed on solid surfaces, where the developing film is observed over months. Further, the characteristic relaxation times would be proportional to R^3, in contradiction with what is observed.

The observed dependence $T_c \propto R$ is consistent with the surface shear viscosity in the film as

the important loss mechanism, provided that the line tension λ does not itself depend significantly on the size of the droplet. Any renormalization due to long-range interactions [2, 22] would decrease the effective line tension with increasing R, increasing the discrepancy between a significant contribution from the bulk viscosity and the size dependence actually observed.

This surface shear viscosity may in principle be measured, either by direct methods such as the canal viscometer or by the effect of surface viscosities on the propagation of capillary waves on a liquid surface. Such studies have been made for PDMS, but neither the canal viscometer [24] nor the study of thermal capillary waves [25] have been able to do more than set an upper bound of 10^{-2} mg/s on such a viscosity, even much above the saturation concentration c_1. Note that if the losses due to the surface viscosity are to dominate over losses in the bulk, $a(\upsilon_s/R\upsilon_b) \gg 1$, where a is the numerical factor ignored in the simple dimensional arguments used here. For $\upsilon_s \sim 10^{-2}$ and $R = 25$ μm, $\upsilon_s/R\upsilon_b \sim 1$. The observed agreement, within the limits of the measurement, with the surface viscosity mechanism suggests that the surface viscosity is near the upper limit.

In so far as one accepts the above model, this does imply an upper bound on the line tension. For the case of concentrations below saturation :

$$\lambda \lesssim 10^{-13}\,\mathrm{N}\,,$$

where again the observed linear dependence on radius favors the upper limit. This is to be compared, under the simplest model for the line tension, to the various interfacial tensions γ in the system (γ[air-PDMS] ≈ 20 mN/m ; γ[PDMS-water] ≈ 40 mN/m), times the thickness of the film d ($d \approx 0.6$ mm) :

$$\gamma d \sim 10^{-11}\,\mathrm{N}\,.$$

This is much larger than the suggested line tension. In a simple bond breaking model, the line tension would be given by

$$k_B\,T/\delta \sim 10^{-11}\,\mathrm{N}\,,$$

if the width δ of the line interface is of the order of the monomer separation, ~ 0.4 nm. Much lower line tensions imply a very diffuse interface.

A more rigorous approach to the three component air-water-polymer system would compare $\lambda A_c^{1/2}$ to the latent heat per molecule L of the gas-to-condensed phase transition, where L can in principle be deduced from the surface pressure π_0 at coexistence of the two phases and the areas per molecule in the two phases A_g and A_c, *via* the Clapeyron relation $L = T\,\dfrac{d\pi_0}{dT}\,(A_g - A_c)$. Unfortunately π_0 is unmeasurably low for the system, with no concomitant indication of the value for A_g.

We are aware of only one other attempt in the literature to deduce a line tension of a monolayer domain, in a very different system consisting of a solid domain in a NBD-stearic acid monolayer : line tensions were suggested to be ~ 10^{-11} N [26], again much larger than our values. The very low surface tensions we deduce are however consistent with the observation that instabilities in the domain boundaries could develop, under apparently minor changes in experimental conditions.

Seul [22] observed similar instabilities in a mixture of a phospholipid and cholesterol, which shows a miscibility gap at room temperature, approaching a consolute point as surface compression is increased. As the compression was increased, he observed shape instabilities on round domains, and at sufficient high compressions, total destabilization of such domains. He demonstrated that the amplitude of modes on the round domains decreased in

wavenumber as q^2, as expected if the energy of the excitation is described by a capillary wave Hamiltonian, i.e., the energy of an excitation is given by the increase in domain length. Somewhat surprisingly, he has not chosen to estimate a (renormalized) domain wall energy as a function of compression from his results and in fact gives all amplitudes in an arbitrary length scale.

It is possible to estimate the line tension at which such effects become observable in domains of the size he shows, $R \sim 25$ μm. The increase in energy of a domain of radius R due to a fluctuation of wavenumber q ($= n/R$; n integer) and amplitude $\xi_q \ll R$ is

$$\Delta E = \lambda \frac{\pi}{2} R q^2 \xi q^2$$

so that by the equipartition theorem

$$\overline{|\xi_q|^2} = \frac{k_B T}{\lambda \frac{\pi}{2} R q^2}$$

If we take $(\sum_q \overline{|\xi_q|^2})^{1/2} \sim R/10$ as a typical value at which the deformations become evident, the associated line tension is

$$\lambda \sim 10^{-14}\,\mathrm{N}$$

about a tenth of our upper limit for the line energy, consistent with the observation that the PDMS system is near, but above, a threshold.

The deformations that Seul observes are consistent with thermal distortion of round domains, and individual modes decay in time, where the decay time can in principle be related to the dissipation that occurs in transport of the domain molecules (surface viscosity, surface diffusion...) The balance between line tension and long-range electrostatic forces can give rise to a permanent distortion. Vanderlick and Möhwald [17] suggest that the critical radius at which these appear gives the line energy, if the relative dipole moment of the domains can be determined by surface potential measurements. Since domains are observed to be deformed in the presence of other domains, this is not at present possible here, but the observation of relaxation suggests 100 μm as a lower limit on R_c. As discussed earlier, this corresponds to a lower limit of 2×10^{-13} N on the line tension λ. This is consistent with the estimate from the relaxation times, $\lambda \sim 10^{-13}$ N and the further observation that relatively little (placing a cover) needs to be done to change the surface configuration.

It should be noted that the relaxation times depend little on the molecular weight of the polymer. Since line tensions are expected to be independent of polymer mass, as surface tensions are as long as this mass is not too small, this suggests that the polymer is not entangled on the surface and that it is the interaction at short distance, between monomer units, which determines the viscosity in the surface. A similar lack of molecular mass dependence has been observed in the monomolecular spreading of the polymer on a solid, silicon [27].

The relaxation times do depend on the polymer sample, with T_c for the polydisperse samples about twice that in the narrow-weight fractions. It is difficult to imagine a mechanism for a difference in surface viscosity when no dependence on molecular mass is observed, suggesting that the line tension is reduced by half in the polydisperse case. A decreased impurity level in the narrow-weight fractions relative to the polydisperse samples is unlikely since the same commercial polydispersed series served as the base [13]. The polydisperse samples do include low molecular weight species, associated with significantly lower surface

tensions. Migration of the lower weight molecules to the borders could lead to lower line tensions. It should be noted that it was with the polydisperse sample that the destabilization of domain borders, upon covering the sample, was observed.

The relaxation after coalescence in the high-density collapsed film is also linear, showing no dependence on the polymer molecular weight. It should be noted that the data here refer to a small number of experiments, two with the high molecular weight (monodisperse) sample and only one with that of low mass (polydisperse), and that in all cases the contrast between domains as well as the background illumination were qualitatively similar. All possible domain classes may not follow the same relaxation law, and for domains of different thicknesses, would not be expected to do so.

The physical situation is much less clear in this case : the polymer may be arranged in multilayers, or the film may consist of regions in which the polymer takes on completely different configurations. The rearrangement of the system under relaxation is not clear. Even the difference in height between domains is presently unknown, though from the low contrast it is unlikely to be much more than one or two polymer layers (0.7-1.5 nm)[3]. It seems unreasonably daring to discuss the viscous processes involved without further information. Experimentally, we find characteristic relaxation times that are 5 times greater than in the monolayer case, but still linear in R. This suggests that the surface viscosity still plays the major role, and that either the surface viscosity is increased or the line tension decreased over the submonolayer case. The effective surface viscosity can in fact be expected to be considerably higher because the resistance would be lowest for movement in the entire polymer layer, thicker than in the submonolayer case and on both sides of the domain boundary. The observable roughness of the polymer domain borders in this case (Figs. 5b, 7), as well as the abrupt destabilization of the surface configuration under no obvious external influence (5e, 5f), suggest that the line tension is also lower.

Conclusions.

Separation into phases of different surface density is noted both at low concentrations and above the point of collapse of a polymer monolayer. A variety of domain shapes can be observed including stripe and foam morphologies. Isolated domains relax to an equilibrium circular shape. The exponential relaxation times are assumed to reflect a balance between a line tension and a viscosity ; the observed linear dependence on the radius of the domain, in the range observed, is consistent with the surface shear viscosity as the dominant term. The relaxation times depend little on the molecular weight of the polymer. This suggests that the polymer does not entangle on the surface and that forces between monomer units are the major contribution to the surface viscosity.

For the monolayer case, the relaxation times, in combination with the very low measured surface viscosities, suggest very low line tensions, less than $\sim 10^{-13}$ N. The further criteria provided by the form of the relaxation time dependence on domain size, which implies that the viscous losses in the layer dominate viscous losses in the bulk, and by the observation that line tension effects dominate electrostatic long-range repulsion in the range of domain sizes observed, both suggest that line tensions λ must be at the upper limit of this range, $\lambda \sim 10^{-13}$ N. An instability in the domain shapes, under apparently minor changes in experimental conditions, is consistent with this interpretation.

While the low line tensions are consistent with all observed physical phenomena, their origin is unclear. They do not reflect a close approach to a critical point ; there is at least a factor of ten density difference between dense and dilute domains.

The observation of domains of contrasting thickness at high concentrations contradicts the long-standing hypotheses of polymer monolayer collapse : it is not a continuous transition to a

bulk phase. The observation of several different discrete film thicknesses in the same layer and the dependence of the configuration on the spreading solution suggests very slow equilibration within the layers and little energy difference between a series of discrete possible configurations.

Polymer molecular layers provide a rich field for further study, for which the dynamics of various processes within the layers are within the reach of present instrumentation. The Brewster Angle Microscope is a particularly method in this context.

Acknowledgements.

This work was supported in part by Rhône-Poulenc ; we are grateful to G. Schorsch and A. Pouchelon for the gift of silicone oils and for many useful discussions. We also thank L. Léger and P. Silberzan for the gift of the narrow weight fraction oils and for sharing their experience and insight into the behavior of PDMS on solid surfaces.

Appendix.

Beginning with the first direct observation of two-phase monolayer systems, large-scale superstructures in the form of stripe and hexatic phases have been observed. The pioneering work of Andelman *et al.* [2] recognized that such phases can result from the competition between line energies, tending to reduce the length of domain boundaries, and long-range electrostatic repulsion. Unfortunately, estimates for neither of these forces, upon which the scale of the structure is exponentially sensitive, have been available to connect this theory to actual observations.

In this paper we make a direct, independent estimate of the line energy for one monolayer system (limited by insufficient knowledge of the surface viscosity). An electrostatic energy would originate in the repulsion between monomer dipoles oriented on average vertically to the interface by the presence of that interface, but the lack of knowledge both of the precise molecular conformation and of the dielectric constant through the interfacial region precludes any estimate from molecular properties. The change of the surface potential in the presence of the dipoles, ΔV, can be measured. It is the purpose of this appendix to show that, for dipolar molecules forming a laterally isotropic phase at a dielectric interface, the long-range electrostatic repulsion can be directly estimated from this measurement, with little ambiguity as to the dielectric constant in the interfacial region.

The electrostatic interactions between dipoles depend both on their orientation and on their environment ; both may be difficult to determine for an amphiphilic molecule at an interface. The molecule is of finite extent with respect to the interfacial region over which the effective dielectric constant (itself dependent on the presence of the monolayer) varies, and different portions of the molecule will feed different dielectric constants of unknown value. Since here we are dealing with a polymer, one can imagine multiple configurations for this polymer, including looping into the substrate (although neutron reflectivity studies of PDMS on water demonstrate a thin, relatively dense layer [3]). All these uncertainties hinder any attempt to deduce the electrostatic interactions from known molecular dipole moments.

Putting the question of exact values aside, in a first approximation, one can consider the layer as having an average dipole moment density μ in a medium of some average dielectric constant. Assuming that the monolayer forms an isotropic fluid, this average dipole moment has no horizontal component, but may have a vertical component since amphiphilic molecules may be oriented with respect to an interface. In treating the total interaction energy, it is convenient to consider a collection of vertical dipoles p, but these refer back to the average dipole density, or more accurately the average differential dipole density between domains ($\Delta\mu = p\,\Delta n$ where Δn is a differential dipole density).

Within the context of this model, the critical radius above which domains are expected to be elongated rather than round is given by Keller *et al.* [16] as

$$R_c = \frac{e^{10/3}\,\delta}{4}\, e^{4\,\pi\varepsilon^{\dagger}\,\lambda/\Delta\mu^2} \quad \text{(in SI units)} \tag{A1}$$

where δ a typical molecular dimension, λ is the line tension, and it is further assumed that the dipole plane is in a medium of uniform dielectric constant $\varepsilon^{\dagger}$. This critical radius reflects the balance between the line energy and the repulsive interaction between the dipoles ; in the model this is given by interaction energy between two individual dipoles p assumed to be aligned, perpendicular to the axis between them, in such a medium :

$$g(r) = \frac{1}{4\,\pi\varepsilon^{\dagger}\,r^3} p^2 \tag{A2}$$

The dipole moment density of a domain is difficult to relate to the molecular dipole moment. On the other hand, the change in surface potential, ΔV, due to the presence of the molecules can be measured directly. Assuming that the dilute phase has the same dipole density as the pure water surface,

$$\Delta\mu = \varepsilon^* \Delta V \tag{A3}$$

in analogy with a parallel plate capacitor, where here ε^* is simply the local dielectric constant felt by the dipoles.

Before using this to deduce a critical radius, or to deduce a line tension if a critical radius is observed as is suggested by Vanderlick and Möhwald [17], one should note that equation (A1) does not apply directly in that the long-range interaction between two dipoles in a real interface depends not only on the local dielectric constant but on the dielectric constant throughout the interfacial region. If one naively sets $\varepsilon^{\dagger} = \varepsilon^*$, one is left with an unknown factor ε^* in expression (A2) for the interaction energy, but this does not necessarily appear in a more complete treatment.

A somewhat more applicable model is given by Andelman *et al.* : the collection of dipoles are considered to lie on one side of an abrupt interface [2]. The result is an interaction energy that can be given directly in terms of the surface potential :

$$g(r) = \frac{1}{2\,\pi r^3}\left(\frac{p}{\varepsilon^*}\right)^2 \frac{\varepsilon_0\,\varepsilon}{\varepsilon_0+\varepsilon} = \frac{1}{2\,\pi r^3}\left(\frac{\Delta V}{\Delta n}\right)^2 \frac{\varepsilon_0\,\varepsilon}{\varepsilon_0+\varepsilon} \tag{A4}$$

Unfortunately, the development of Andelman *et al.* was immediately specialized to the model of dipoles within the bulk water, even in the earlier paper where the interaction energy is given explicitly in terms of this surface potential, and the more general form independent of the choice of water or air for the position of the dipole sheet seems to have been overlooked since.

No surface is abrupt, but the development of the electrostatic interaction energy in terms of a measurable surface potential continues to hold in more realistic models. Consider the following very simple, commonly used model : two bulk phases of dielectric constant ε_0 and ε separated by a thin slab of thickness d and dielectric constant ε^*. As with the single interface, the interaction energy $g(r)$ of two dipoles of individual dipole moment p (perpendicular to the interface) within the thin slab can be easily calculated using the method of images in which an interface is replaced by an image dipole symmetrically placed to that interface [28]. A dipole p' in the film will have an image dipole $p'(\varepsilon_0 - \varepsilon^*)/(\varepsilon_0 + \varepsilon^*)$ above the air-film interface (note that the sign is opposite that for an image charge) and an image dipole $p'(\varepsilon - \varepsilon^*)/(\varepsilon + \varepsilon^*)$ below the film/water interface ; this leads to an infinite series of image dipoles receding from the interface in the equivalent of multiple reflection [29]

but this can simply be summed as long as the distance r between the two real dipoles is very large, $r \gg d$ (the case of interest since we are interested in the energy difference between domain configurations varying on the scale of micrometers and more). Under this assumption, each image dipole relative to one interface is obtained as the sum of the image of p and the image of the image across the other interface, leading to an interaction energy between real dipoles of

$$g(r) = \frac{1}{2\pi r^3}\left(\frac{p}{\varepsilon^*}\right)^2 \frac{\varepsilon_0\,\varepsilon}{\varepsilon_0+\varepsilon}\frac{1}{2\pi r^3}\left(\frac{\Delta V}{\Delta n}\right)^2 \frac{\varepsilon_0\,\varepsilon}{\varepsilon_0+\varepsilon} \approx \frac{1}{2\pi r^3}\left(\frac{\Delta V}{\Delta n}\right)^2 \varepsilon_0\,, \qquad \text{(A5)}$$

where the last approximation holds for the air-water interface for which $\varepsilon \gg \varepsilon_0$. Note that no assumptions are made about the value of ε^* and that, while a very simple model of the interfacial region was used to derive this result, the essential supposition was that it be much thinner than the distance between dipoles. In particular, the same expression can be derived (at the expense of slightly more bookkeeping) for a series of coupled vertical dipoles distributed through the interfacial region ; it is not dependent on the simplified model in which every portion of the amphiphilic molecule feels a single average dielectric constant.

Using this expression for the long-range interaction energy between dipoles at an interface, the result of Keller *et al.* (Eq. (A1)) may be directly transferred to the

$$R_c = \frac{e^{10/3}\,\delta}{4}\, e^{\lambda(2\pi/\varepsilon_0)(\varepsilon^*/\Delta\mu)^2} = \frac{e^{10/3}\,\delta}{4}\, e^{2\pi\lambda/\varepsilon_0 \Delta V^2}. \qquad \text{(A6)}$$

Thus a measurement of the difference in surface potential between domains can be used to estimate the long-range electrostatic contribution to the energy balance, with little of the ambiguity which might be expected with respect to the dielectric constant in the interface and to the configuration of the molecule through that interface. With a determination of the line energy, the predictions of striped and other large-scale structures as well as the shape of individual domains can be compared quantitatively with observations. The major remaining uncertainty is in the appropriate value for the molecular cutoff δ, particularly for a polymer with many different length scales at which a molecular configuration may be imposed. However, the expression for R_c is insensitive to this uncertainty, compared to the exponential error induced by any uncertainty in the ratio $\lambda/\Delta V^2$. Because of the latter uncertainty, it is unlikely that a precise value for R_c can be predicted ; on the other hand, the value of the ratio $\lambda/\Delta V^2$ for which R_c is in the observable range can be predicted quite precisely and any experiment allowing a variation of that ratio would be particularly revealing.

The observation of stripes and similar morphologies suggests comparison of this theory with measured line tensions if the electrostatic forces can be determined for our system. Measurements of the surface potential of PDMS layers with respect to the surface potential of water exist in the literature [19, 6]. Very large electrodes (5 cm × 5 cm) were used, so that averaging over different domains is expected. The dilute domains can be assumed to be equivalent to the pure water surface, while the change in surface potential associated with a dense domain can be taken from the value at saturation of the surface with this phase ; the best estimate of this is the point at which the surface pressure begins to rise significantly. From the data of Bernett *et al.* [19], this leads to the estimate $\Delta V = 0.12$ V. Using $\delta = 0.4$ nm, the distance between monomers in the dense phase estimated from the area per monomer at this same saturation, this determines the relation between the critical radius and the line tension :

$$R_c\,(\text{nm}) \sim 3\, e^{4.9\,\lambda/10^{-13}\,\text{N}} \qquad \text{(A7)}$$

A critical radius of 100 μm, which would be within the scale of the field-of-view of the present microscope, would correspond to a line tension $\lambda = 2 \times 10^{-13}$ N.

References

[1] KNOBLER C., in Advances in Chemical Physics, I. Prigogine, S. A. Rice Eds. **77** (Wiley : New York, 1990) p. 397.

[2] ANDELMAN D., BROCHARD F., JOANNY J.-F., *J. Chem. Phys.* **86** (1987) 3673 ;
ANDELMAN D., BROCHARD F., DE GENNES P.-G., JOANNY J.-F., *C. R. Acad. Sc. Paris* **301 II** (1985) 675.

[3] LEE L. T., MANN E. K., LANGEVIN D., FARNOUX B., *Langmuir* **7** (1991) 3076.

[4] MANN E. K., LANGEVIN D., *Langmuir* **7** (1991) 1112.

[5] SAUER B. B., YU H., YAZDANIAN M., ZOGRAFI G., KIM M. W., *Macromolecules* **22** (1989) 2332.

[6] FOX W., TAYLOR P. W., ZISMAN W. A., *Ind. Eng. Chem.* **39** (1947) 1401.

[7] HESLOT F., CAZABAT A. M., LEVINSON P., FRAYSSE M., *Phys. Rev. Lett.* **65** (1990) 599 ;
SILBERZAN P., LÉGER L., *Phys. Rev. Lett.* **66** (1991) 185.

[8] LÖSCHE M., SACKMANN E., MÖHWALD H., *Ber Bunsenges Phys. Chem.* **87** (1983) 848.

[9] MCCONNELL H. M., TANN L. K., WEISS R. M., *Proc. Natl. Acad. Sci. (USA)* **81** (1984) 3249 ;
WEISS R. M., MCCONNELL H. M., *Nature* **310** (1984) 3249 ;
GAUB H. E., MOY V. T., MCCONNELL H. M., *J. Phys. Chem.* **90** (1985) 1721.

[10] LÖSCHE M., DUWE H. P., MÖHWALD H., *J. Colloid Interface Sci.* **126** (1988) 432.

[11] BERCEGOL H., GALLET F., LANGEVIN D., MEUNIER J., *J. Phys. (France)* **50** (1989) 2277 ;
BERCEGOL H., MEUNIER J., *Nature* **356** (1992) 226 ;
BERCEGOL H., *J. Phys. Chem.* **96** (1992) 3435 ;
MULLER P., GALLET F., *J. Phys. Chem.* **95** (1991) 3257.

[12] HÉNON S., MEUNIER J., *Rev. Sci. Instrum.* **62** (1991) 936 ;
A similar method has been developed independently : HÖNIG D., MÖBIUS D., *J. Phys. Chem.* **95** (1991) 4590.

[13] LÉGER L., SILBERZAN P., Gift.

[14] STINE K. J., KNOBLER C. M., DESAI R. C., *Phys. Rev. Lett.* **65** (1990) 1004.

[15] STINE K. J., RAUSEO S. A., MOORE B. G., WISE J. A., KNOBLER C. M., *Phys. Rev. A* **41** (1990) 6884 ;
BERGE B., SIMON A. J., LIBCHABER A., *Phys. Rev. A.* **41** (1990) 6893.

[16] KELLER D. J., KORB J. P., MCCONNELL H. M., *J. Phys. Chem.* **91** (1987) 6417.

[17] VANDERLICK T. K., MÖHWALD H., *J. Phys. Chem.* **94** (1990) 886.

[18] OWEN M. J., in *Advances in Chemistry Series* **224** Silicon-Based Polymer Science, J. M. Zeigler, F. W. G. Fearon Eds. (American Chemical Society : Washington D. C., 1990) p. 705.

[19] BERNETT M. K., ZISMAN W. A., *Macromolecules* **4** (1971) 47.

[20] TROIAN S. M., WU X. L., SAFRAN S. A., *Phys. Rev. Lett.* **62** (1989) 1496 ;
CAZABAT A. M., HESLOT F., TROIAN S. M., CARLES P., *Nature* **346** (1990) 824.

[21] RICE P. A., MCCONNELL H. M., *Proc. Natl. Acad. Sci. USA* **86** (1989) 6445.

[22] SEUL M., SAMMON M. J., *Phys. Rev. Lett.* **64** (1990) 1903 ;
SEUL M., *Physica A* **168** (1990) 198 ;
SEUL M., SAMMON M. J., *Rev. Sci. Instrum.* **62** (1991) **784.**

[23] LAMB H., Hydrodynamics, 6th Ed. (Cambridge University Press, Cambridge, 1963) p. 641.

[24] JARVIS N. L., *J. Phys. Chem.* **70** (1966) 3027.

[25] HARD G., NEUMANN R. D., *J. Colloid Interface Sci.* **120** (1987) 15.

[26] MULLER P., GALLET F., *Phys. Rev. Lett.* **67** (1991) 1106.

[27] DAILLANT J., *Thesis* (l'Université de Paris-Sud, Orsay, 1989) ;
DAILLANT J., BENATTAR J. J., LÉGER L., *Phys. Rev. A.* **41** (1990) 1963.

[28] JACKSON J. D., Classical Electrodynamics, 2nd edition (John Wiley & Sons, New York, 1975) p. 147ff.

[29] MORSE P. M., FESHBACH H., Methods of Theoretical Physics (McGraw-Hill Book Company, New York, 1953) I p. 814ff.